Pure & Appl. Chem., Vol. 64, No. 6, pp. 789–797, 1992.
Printed in Great Britain.

Exploiting lineshape singularities in ESEEM of orientationally disordered systems

E.J. Reijerse[1] and **S.A. Dikanov**[2]

[1]Department of Molecular Spectroscopy, University of Nijmegen, Toernooiveld, 6525 ED Nijmegen, The Netherlands.

[2]Institute of Chemical Kinetics and Combustion, USSR Academy of Sciences, Novosibirsk 630090, USSR.

ABSTRACT

Experimental strategies are presented to obtain the magnetic interaction parameters of I=1/2 nuclei weakly coupled to paramagnetic species (S=1/2) in orientationally disordered materials: By performing ESEEM experiments as a function of the microwave frequency it is possible to induce lineshape singularities either in the basic modulation features due to the primary nuclear spin transitions or in the sum and difference "combination" lineshapes which are generated using 2-pulse and 4-pulse ESEEM techniques. The position of these lineshape singularies can be easily interpreted in terms of hyperfine parameters using analytical expressions.

The analysis of the basic and combination lineshape singularities can also be extented to two-dimensional 4-pulse ESEEM (HYSCORE) experiments. In this case the combination lines are replaced by mountain ridge shaped correlation features in the two-dimensional frequency domain. Like the combination lines the correlation feature can be classified as sum (Zeeman dominated) and difference (Hyperfine dominated) features. Furthermore, it is demonstrated that two-dimensional techniques are very powerfull in disentangling broad and complicated spectral features due to overlapping basic lineshapes or to different interacting nuclei.

INTRODUCTION

The interpretation of powder FT-ESEEM spectra in terms of interaction parameters is complicated for several reasons: On one hand, anisotropic interactions (hyperfine and quadrupole) lead to deep modulation effects, but on the other hand the spectral features are broadened and deformed by the anisotropic behaviour of the modulation intensity. Therefore, the spectral features no longer assume the familiar powder lineshape reflecting the angular probability distribution, but are instead a complicated function of both the angular distribution and the anisotropic modulation intensity. The situation can be further complicated by the overlap of the broad lineshapes with each other.

To eleviate this problem many groups have performed numerical line shape calculations of the basic modulation features for the S=1/2, I=1/2 system as a function of the hyperfine parameters [1–5]. In particular the recent study by Lai et al. [6] provided an exhaustive analytical treatment of the lineshape for the basic frequencies as a function of the isotropic hyperfine parameter, a, the perpendicular component of the (pseudo) dipolar hyperfine matrix ($T_\perp$), and the external magnetic field. This multifrequency analysis was carried out for the condition $|T_\perp/a| \leq 0.4$, i.e. a dominating isotropic contribution to the hyperfine interaction. A general conclusion of this study is that individual lineshape singularities can be induced by matching the nuclear Larmor frequency to the corresponding principal values of the hyperfine matrix: $\nu_I = |\frac{1}{2}A_{x,y,z}|$.

Other studies [7] showed that, in the limit of a small hyperfine interaction, the position of the sum combination line is mainly determined by the anisotropic part of the hyperfine interaction. It may, therefore, give an independent handle to the determination of the dipolar interaction ($T_\perp$). The recent study of Reijerse and Dikanov [8] combined both mentioned strategies and provided an overall analytical description of the lineshape singularities for any combination of hyperfine parameters.

In this paper this general strategy will be summarized and extensions to 2D-ESEEM (HYSCORE) techniques will be discussed.

THEORY

The spin Hamiltonian for an S=1/2 I=1/2 system is written in the strong field approximation as:

$$H/h = \nu_S S_z + A S_z I_z + B S_z I_x - \nu_I I_z. \tag{1}$$

Parameters A and B are the secular and nonsecular contributions of the hyperfine interaction to the spin Hamiltonian. The hyperfine interaction is taken axial with isotropic component, a, and principal values $(-T, -T, 2T)$. Parameters A and B are now expressed as:

$$A = a + T(3\cos^2\theta - 1)\ ;\ \ B = 3T\sin\theta\cos\theta \tag{2}$$

θ is the angle between the dipolar HFI tensor axis and the direction of the external magnetic field. Using these parameters the primary ESEEM for an electron-nuclear spin system with S=1/2 and I=1/2 can be expressed as:

$$V(\tau) = 1 - \frac{k}{2}[1 - \cos 2\pi\nu_\alpha\tau - \cos 2\pi\nu_\beta\tau + \frac{1}{2}\cos 2\pi(\nu_\alpha + \nu_\beta)\tau + \frac{1}{2}\cos 2\pi(\nu_\alpha - \nu_\beta)\tau] \tag{3}$$

where

$$\nu_{\alpha(\beta)}(\theta) = \left[\left(\nu^2_{\|\alpha(\beta)} - \nu^2_{\perp\alpha(\beta)}\right)\cos^2\theta + \nu^2_{\perp\alpha(\beta)}\right]^{1/2} \tag{4}$$

$$\begin{aligned} \nu_{\|\alpha(\beta)} &= -\nu_I \pm \tfrac{a+2T}{2} \\ \nu_{\perp\alpha(\beta)} &= -\nu_I \pm \tfrac{a-T}{2} \end{aligned} \tag{5}$$

The modulation depth parameter, k, is usually written in the form [9]:

$$k = \left(\frac{\nu_I B}{\nu_\alpha \nu_\beta}\right)^2 \tag{6}$$

For orientationally disordered systems, where the external magnetic field is randomly oriented relative to the HFI tensor axes, the line shapes for the basic frequencies $\nu_{\alpha(\beta)}$ are determined by the orientational dependence of the line positions $\nu_{\alpha(\beta)}(\theta)$, their intensities $k(\theta)$, and the statistical weight factor: $\frac{1}{2}\sin\theta d\theta$. The complete lineshape function for the $\nu_{\alpha(\beta)}$ lines in a powder spectrum is given by:

$$I(\nu)_{\alpha(\beta)} = \frac{1}{4}k(\theta)\sin\theta \left|\frac{\partial\theta}{\partial\nu_{\alpha(\beta)}}\right| \tag{7}$$

which can be evaluated further as:

$$I(\nu)_{\alpha(\beta)} = \frac{k(\theta)\ \nu(\theta)_{\alpha(\beta)}\ (1/\cos\theta)}{12|T[(2a+T)/4 \mp \nu_I]|} \tag{8}$$

Basic frequencies

Analysis of eq. 8 immediately shows why in ESEEM the powder lineshapes are lost: At the principle orientations $(\theta = 0, \pi/2)$ the modulation depth parameter, k, drops to zero thus suppressing the intensity at the canonical positions. It has been demonstrated [6,8] that the intensity at the canonical positions can be recovered by adjusting the Zeeman frequency such that the energy splitting in one of the m_S manifolds is "cancelled", i.e. $\nu_{\perp\alpha(\beta)} = 0$ or $\nu_{\|\alpha(\beta)} = 0$. In particular the itensity of the $(\perp)$ features will be enhanced substantially due to the favourable statistical weight $(\cos\theta)$ for this orientation. In Table 1 the cancellation conditions and the related maxima are summarized.

Table I. Maxima and singularities for basic frequencies

condition	$\nu_{\perp\alpha}$	$\nu_{\perp\beta}$	condition	$\nu_{\|\alpha}$	$\nu_{\|\beta}$
$\nu_{\perp\alpha} = 0$	Max*	Singularity	$\nu_{\|\alpha} = 0$	–	Max
$\nu_{\perp\beta} = 0$	Singularity	Max*	$\nu_{\|\beta} = 0$	Max	–

(*) The maximum intensity of this feature occurs at zero frequency

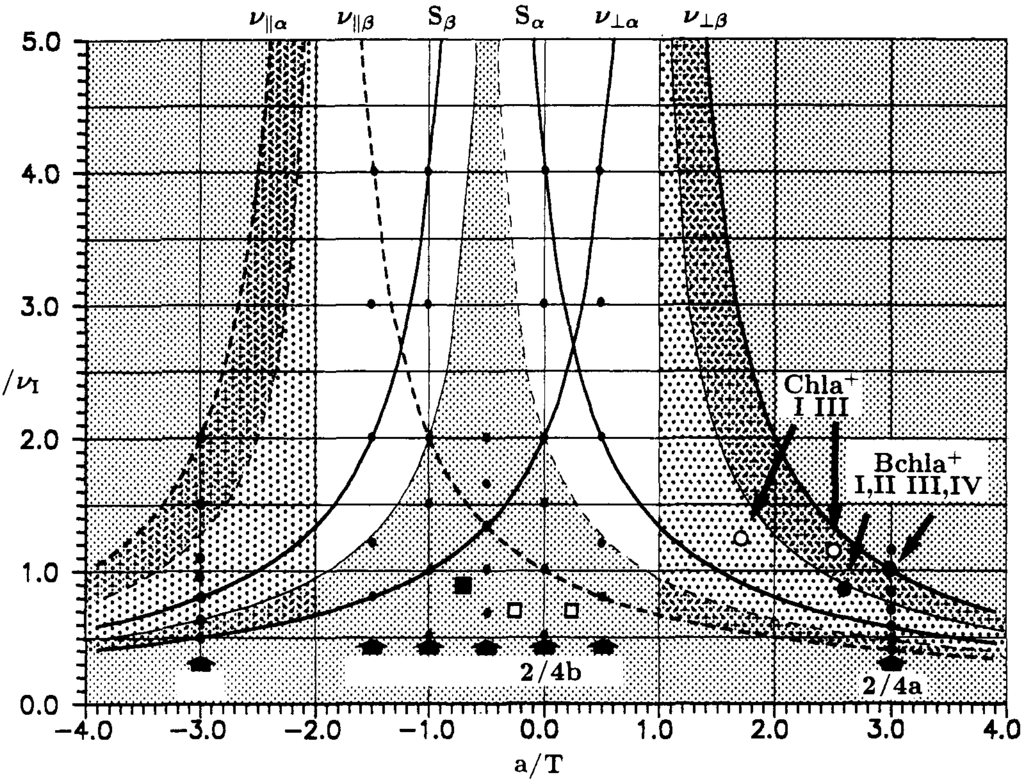

Figure 1: (After fig. 1 from ref. [8]) Graphical representation of the conditions for which lineshape singularities are observed for the basic α and β features. The conditions, which are explained in the text, are either related to the $\|$ orientation (dashed curves: $\nu_{\|\alpha}$ and $\nu_{\|\beta}$), to the $\perp$ orientation (solid curves: $\nu_{\perp\alpha}$ and $\nu_{\perp\beta}$), or to a special singularity (solid curves: S_α and S_β). For negative values of (T/ν_I) an identical representation can be drawn in which the α and β indices are interchanged. The weakly shaded areas in the corners of the graph represent the (a, T, ν_I) parameter space for which the difference combination line $(\nu_\alpha - \nu_\beta)$ is observed, whereas the central shaded area indicates the same for the sum combination line $(\nu_\alpha + \nu_\beta)$. The coarsely shaded areas represent the parameter space for which the "matching range" of the individual α and β features can be exploited according to the study of Lai et. al. [6]. Also indicated are the experimental parameters of some selected systems: [○] Chla+ nitrogens I&III [10]; [○] Bchla+ nitrogens I,II & III,IV [11]; [□] Silver atoms [12]; [■] Trapped electrons [13].

Apart from the maxima and singularities which occur for the "cancellation" conditions, inspection of equation (8) also shows that a lineshape singularity is induced for the condition $\nu_I = \pm(2a+T)/4$ independent of the angle θ. An isotropic line is observed at a frequency of $\frac{3}{4}T$. This singularity is connected with the derivative $\partial\nu_{\alpha(\beta)}/\partial\theta = 0$ *for all* θ when $\nu_{\perp\alpha(\beta)} = -\nu_{\|\alpha(\beta)} = \mp\frac{3}{4}T$. In figure 1 the conditions to observe the basic lineshape singularities are graphically represented. For generality reasons the dimensionless parameters (a/T) and (T/ν_I) have been used to express the cancellation conditions:

$$\begin{array}{ll} \nu_{\perp\alpha(\beta)} = 0: & (T/\nu_I) = \pm\frac{2}{(a/T)-1} \\ \nu_{\|\alpha(\beta)} = 0: & (T/\nu_I) = \pm\frac{2}{(a/T)+2} \end{array} \tag{9}$$

The condition for the single line singularity $S_{\alpha(\beta)}$ at $\frac{3}{4}T$ is given by:

$$S_{\alpha(\beta)}: \quad (T/\nu_I) = \pm\frac{4}{2(a/T)+1} \tag{10}$$

It was demonstrated by Lai. et. al [6] that one can always determine a range of ν_I in which the k parameter attains its maximum value for a specific orientation: $k(\theta) = 1$ independent of the value of B (as long as $B \neq 0$). This condition is fulfilled when the nuclear Zeeman interaction "matches" the magnitude of the effective hyperfine interaction [6,8], i.e. $\nu_I = \frac{1}{2}\sqrt{A^2+B^2}$. The coarsely shaded areas in fig. 1 represent the "matching range" which is bounded by the cancellation conditions.

Combination frequencies

In 2-pulse and in 1D 4-pulse ESEEM experiments, apart from the basic nuclear transition frequencies $\nu_{\alpha(\beta)}$ also combination lines $\nu_\alpha \pm \nu_\beta$ occur. In contrast to the basic frequencies, the frequency position of the combination lines can have an extra singularity $(\partial(\nu_\alpha \pm \nu_\beta)/\partial\theta = 0)$ at an angle θ different from 0 or $\pi/2$. Since the modulation intensity will *always* remain finite at this angle, a real lineshape singularity will emerge.

The expression of the peak position of these singularities is, however, identical for both the sum and the difference combination line [8]:

$$(\nu_\alpha \pm \nu_\beta)_{max} = 2\nu_I \left(1 + \frac{9/16\ T^2}{\nu_I^2 - (T+2a)^2/16}\right)^{1/2} \tag{11}$$

The condition $|T + 2a| < 4\nu_I$ or $|T + 2a| > 4\nu_I$ will distinguish between the sum and difference combination line. The central shaded area in fig. 1 represents the combinations of a, T and ν_I for which the singularity of the combinations line $(\nu_\alpha + \nu_\beta)$ is defined. The shaded areas in the corners of fig. 1 represent the parameter space for which the difference combination line is observed.

EXPERIMENTAL STRATEGIES

The graphs in fig. 1 provide a very useful way to map spectral data of various paramagnetic species and to predict which spectral features will be enhanced upon variation of the external magnetic field. As an example we mapped the ^{15}N-hyperfine parameters obtained for some photosynthetic materials (see figure caption). In a multifrequency experiment the points which represent a given set of hyperfine values (a/T and T/ν_I) will shift along a vertical line thus crossing several curves indicating either singularity conditions or conditions that bound the area for which the combination lines are observable.

Dominating isotropic hyperfine interaction

In fig. 2 we present a series of simulations of primary ESEEM (amplitude) spectra as a function of the (T/ν_I) parameter for two different values of the (a/T) parameter. We will now discuss fig. 2a which shows the series for $(a/T) = 3.0$: In the *weak coupling range* $(T/\nu_I = 0.2)$ the basic frequencies are near their isotropic value while the sum combination line is quite strong and peaks near the double Zeeman frequency. Upon increasing (T/ν_I), the β feature will be weighed towards the $\|$ canonical position. The position of the combination line is described by eq. (11). For $(T/\nu_I) = 0.4$ the β feature peaks exactly at the $\nu_{\|\beta}$-position. This maximum, like any peak caused by a cancellation condition, is positioned at a frequency of $2\nu_I$. Proceeding further the β feature broadens out and the sum combination line disappears. Instead, the α lineshape attains a singularity at $(T/\nu_I) = 0.571$. Going to stronger coupling, starting at $(T/\nu_I) = 0.8$, the β shape is weighed towards the $\perp$ canonical position while the difference combination line pops up. At point $(T/\nu_I) = 1.0$ the β shape peaks exactly at the $\perp$ canonical position $(\nu_{\perp\beta} = 2\nu_I)$. In the strong coupling range only the difference combination line and the β shape (still slightly weighed towards the $\perp$ position) are visible.

In the region given by $-2 < (a/T) < 1$ the α and β features are no longer separated in the FT-ESEEM spectrum and the difference combination frequency is no longer visible. According to fig. 1, this range is the exclusive domain of the sum combination frequency, which is symmetric around $(a/T) = -0.5$. At this ratio, for any value of the Larmor frequency the sum combination feature will be observed. Fig. 2b, shows a series of spectral simulations for $(a/T) = 0$. It is demonstrated that the lineshape enhancement strategy of varying ν_I may still be successful. The edge singularities of the ν_α feature at $(T/\nu_I) = 2.0$ and the $S_{\alpha(\beta)}$ line singularity at $(T/\nu_I) = 4.0$ are very pronounced.

Extension to 2D-ESEEM

Recently, the 2D-HYSCORE technique [14] was applied for the first time on disordered materials [15, 16]. It turned out that the specific properties of this technique offer many advantages over the conventional 3-pulse 2D ESEEM technique. The basic pulse sequence of the HYSCORE experiment is displayed in figure 3. The echo signal can be regarded as a 4-pulse stimulated echo [14]. For every spectrum the echo is recorded in a two-dimensional time domain as a function of both waiting time t1 and t2. Since during both these waiting times the relevant electron spin coherence is stored along the magnetic z-axis, the main cause of echo decay will be the spin-lattice relaxation time. Therefore,

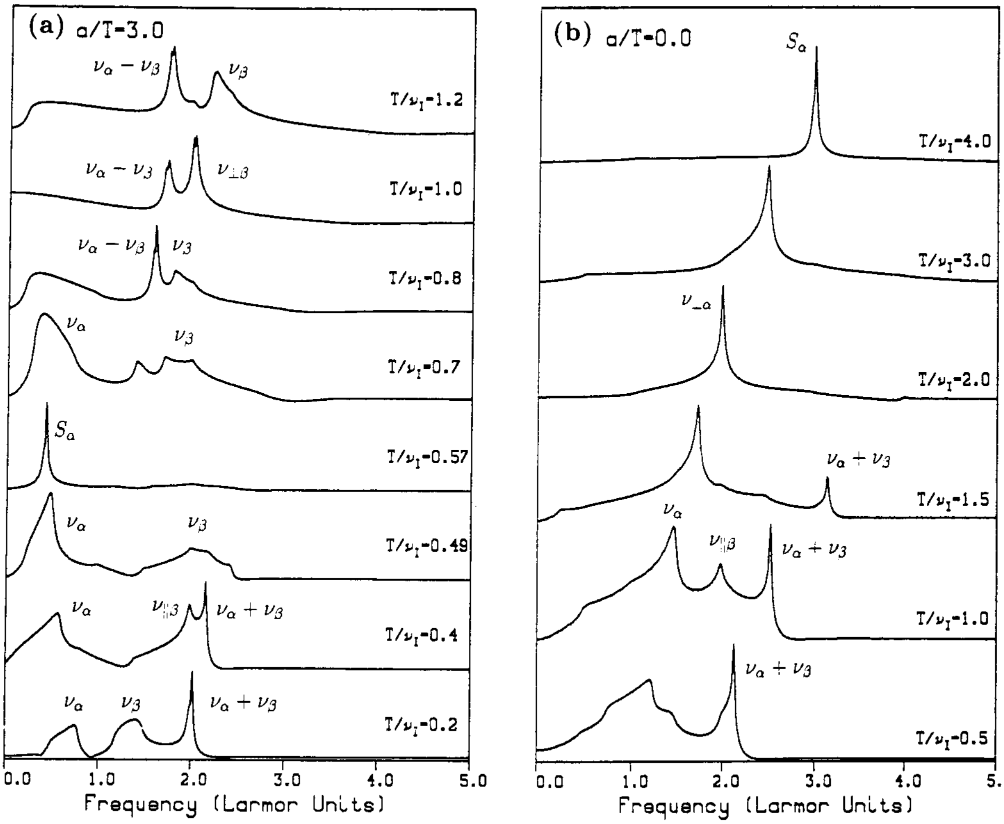

Figure 2: Simulated primary FT-ESEEM amplitude spectra for (a) the case: $(a/T) = 3.0$ and (b) the case: $(a/T) = 0$. No dead time effects are included. All spectra are scaled to full scale.

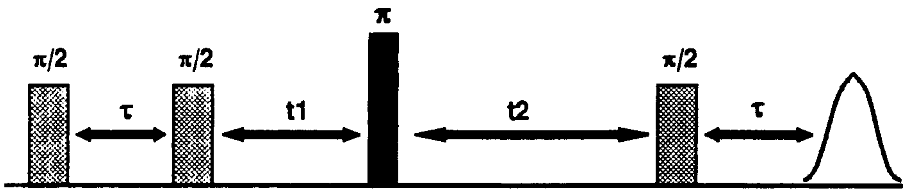

Figure 3. Basic pulse sequence of 4-pulse echo experiment

as compared to the 3-pulse 2D-ESEEM experiment, where during waiting time τ the spin-spin relaxation time is active, the spectral resolution in the second dimension ("t1" for the HYSCORE experiment) is substantially improved. However, in order to avoid interference of unwanted echoes with the stimulated 4-pulse echo, extensive phase-cycling is necessary [17]. Also, the 2D-FT pattern will be dependent on the fixed waiting time τ, which may induce "blind spots" in the modulation pattern. The general expression for the echo envelope of the 4-pulse stimulated echo is given by:

$$E(\tau, t1, t2) = R_2(\tau) R_1(t1 + t2) S(\tau, t1, t2) \tag{12}$$

where $R_{1,2}$ are the relaxation decays caused by T1 and T2 relaxation.
$S(\tau, t1, t2)$ is the modulated part of the echo:

$$\begin{aligned} S(\tau, t1, t2) &= \sum_{ijklmn} M_{il} M_{lj}^{\dagger} M_{jm} M_{mk}^{\dagger} M_{kn} M_{ni}^{\dagger}\, e^{-\omega_{ij}\tau} e^{-\omega_{ik} t2} e^{-\omega_{ln}\tau} e^{-\omega_{lm} t1} \\ &+ \sum_{ijklmn} M_{il} M_{lj}^{\dagger} M_{jm} M_{mk}^{\dagger} M_{kn} M_{ni}^{\dagger}\, e^{-\omega_{ik}\tau} e^{-\omega_{jk} t1} e^{-\omega_{ln} t2} e^{-\omega_{mn}\tau} \\ &+ C.C. \end{aligned} \tag{13}$$

Where M represents the matrix of EPR transition probabilities between the nuclear spinlevels in the α manifold (ijk) and the β manifold (lmn). For the spin system S=1/2 I=1/2 the above expression will reduce to the recently derived by Gemperle et al. [17]. The signal contribution exclusively due to the correlations between the α and β features is given by:

$$\begin{aligned} S(t1,t1) = \ & \tfrac{k}{4}C[\ c^2\cos(\omega_\beta t2 + \omega_\alpha t1 + \delta_+) \\ & + \ s^2\cos(\omega_\beta t2 - \omega_\alpha t1 - \delta_-) \\ & + \ c^2\cos(\omega_\alpha t2 + \omega_\beta t1 + \delta_+) \\ & + \ s^2\cos(\omega_\alpha t2 - \omega_\beta t1 - \delta_-)] \end{aligned} \tag{14}$$

$\delta_\pm$ are phase factors depending on τ. Concentrating on the t1 dependence of the signal due to $\cos(\omega_\beta t2)$ we observe that the two phase modulated contributions $\cos(\omega_\beta t2 + \omega_\alpha t1)$ and $\cos(\omega_\beta t2 - \omega_\alpha t1)$ have different amplitudes:

$$\begin{aligned} s^2 = \cos^2(\delta/2) &= \left|\frac{\omega_I^2 - (\omega_\alpha + \omega_\beta)^2/4)}{\omega_\alpha\omega_\beta}\right| \\ c^2 = \cos^2(\delta/2) &= \left|\frac{\omega_I^2 - (\omega_\alpha - \omega_\beta)^2/4)}{\omega_\alpha\omega_\beta}\right| \end{aligned} \tag{15}$$

Therefore, in contrast to the 3-pulse 2D ESEEM experiment, the HYSCORE 2D-FT spectra will reveal the sign of the phase modulation which will yield extra information about the coupling parameters of the spin system.

It is important to note that the 2D-HYSCORE spectra can be interpreted without knowledge of the mechanisms behind the experiment. Exactly like in 3-pulse 2D-ESEEM the nuclear spin transitions in the two m_S manifolds are correlated to each other by crosspeaks in the 2D-frequency domain. In case of powder spectra, the correlation peaks may become "ridges". In order to get a more basic understanding of the potential use of 2D techniques in the study of disordered materials we performed several numerical HYSCORE simulations of the spin system S=1/2 I=1/2 using the multifrequency approach discussed in the previous sections. The 2D series presented in figure 4 and 5 are generated using the same parameters as the 1D series displayed in figure 2.

For the $(a/T) = 3.0$ series the correlation features are, like 1D basic $\nu_{\alpha(\beta)}$ lineshapes, separated from each other. The correlation lineshapes form mountain like ridges perpendicular to the main diagonal. The sum combination frequency (which in the 1D spectra contains a singularity) can be inferred from the 2D picture by taking the projection of the correlation features on the main diagonal. Sliding up the line $(a/T) = 3.0$ in the "modulation map" (fig. 1) we observe that the correlation ridges become more extended and somewhat distorted by "second order effects", i.e. the mountain ridge will be "bended" slightly. In the 1D picture this is translated in terms of the sum combination feature which is now shifted from the "first order" double Zeeman value $(2\nu_I)$. The cancellation condition $\nu_{\perp\alpha} = 0$ at $(a/T) = 0.4$ can be easily recognized in the 2D picture since the correlation ridges "touch" the main frequency axes (f1,0), (0,f2). The special singularity S_α is represented in the 2D picture by the correlation ridges which are now parallel to the main frequency axis. The cancellation condition $\nu_{\|\alpha} = 0$ is less pronounced because of the unfavourable statistical weight factor for the $\|$ orientation but, again, it can be observed that the ridges "touch" the main frequency axes. Finally, in the strong coupling region, the correlation ridges are oriented parallel to the anti-diagonal of the 2D frequency domain.

It is striking to observe the redistribution of intensity of the correlation features over the two sets of frequency quadrants: In the weak coupling range positive phase modulation dominates which leads correlation features in the $(+,+)/(-,-)$ quadrants. In the intermediate coupling range the intensity is distributed equally over the $(+,+)/(-,-)$ and the $(+,-)/(-,+)$ quadrants, while in the strong coupling range negative phase modulation is dominating leading to correlation features in the $(+,-)/(-,+)$ quadrants. Furthermore, the correlation features can be classified as sum features (in the weak coupling range), and difference features (in the strong coupling range). A similar behaviour is observed for the $(a/T) = 0$ series presented in figure 5.

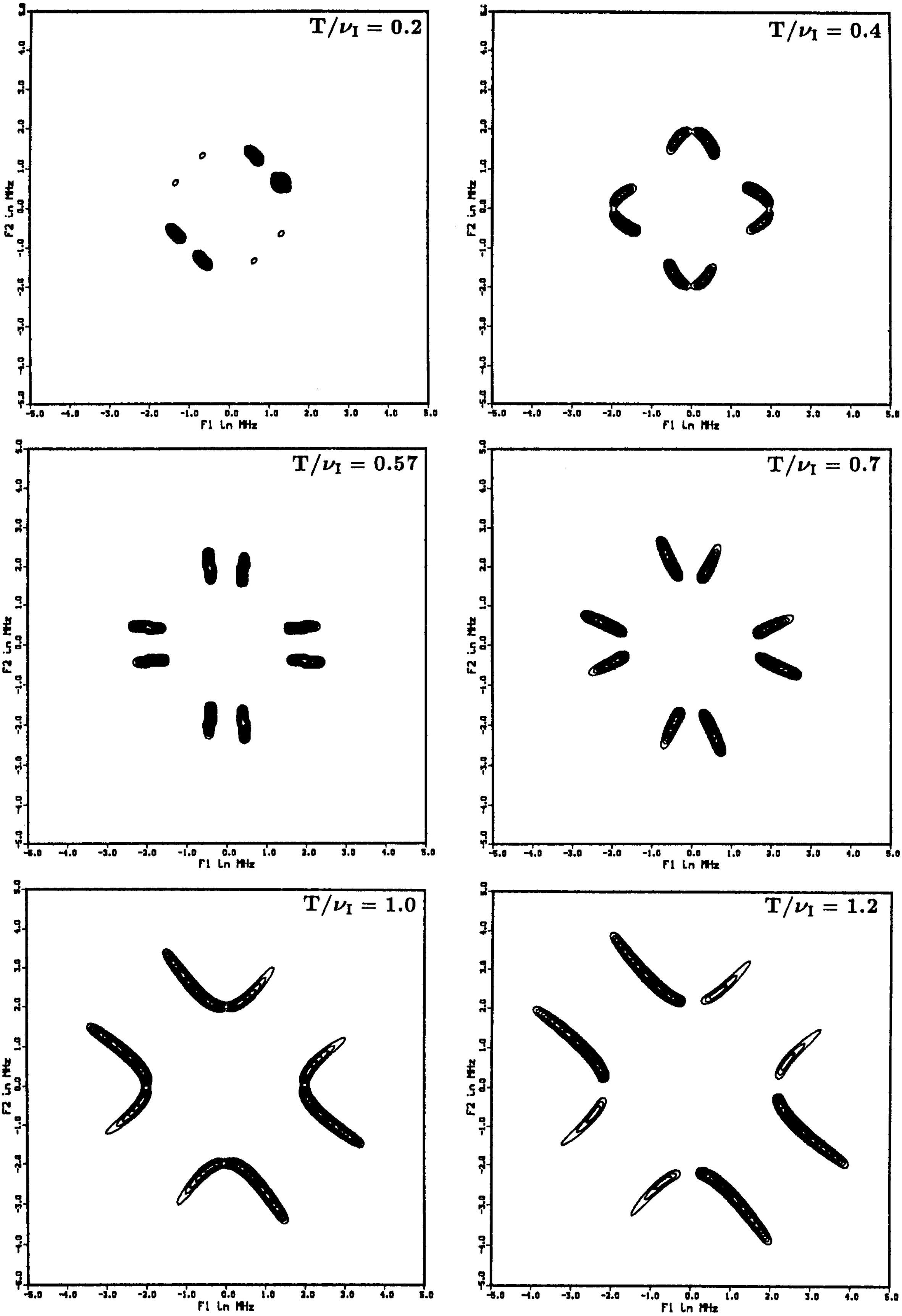

Fig. 4 2D-HYSCORE simulations for the case $(a/T) = 3.0$.

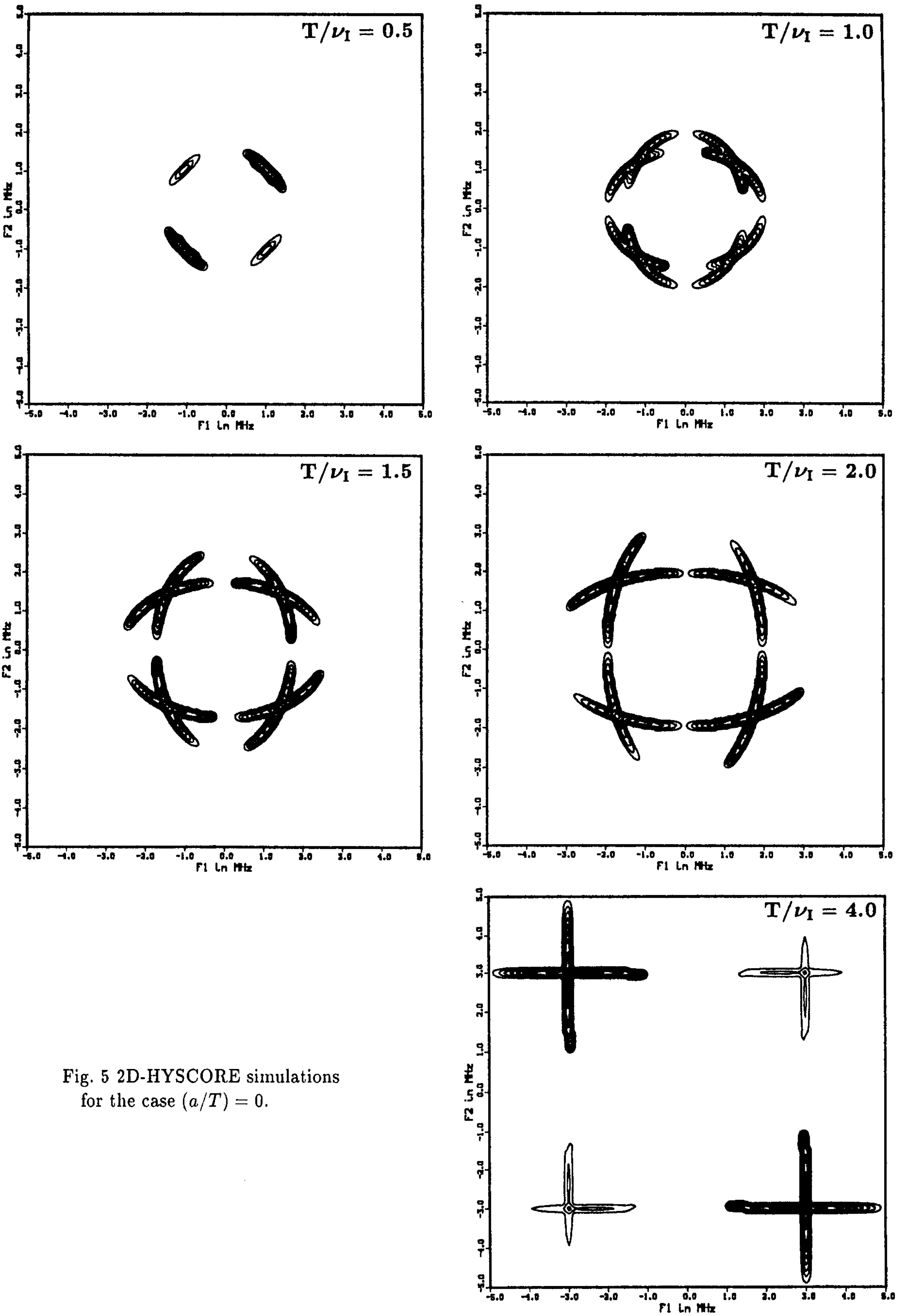

Fig. 5 2D-HYSCORE simulations for the case $(a/T) = 0$.

CONCLUDING REMARKS

We have demonstrated that 2-pulse ESEEM will always show features, either basic frequencies or combination lines, which can be interpreted using analytical expressions. Multi-frequency strategies enable full use of these expressions.

The observed singularities can be readily translated into 2 dimensions and the preliminary HYSCORE simulations show that important information can be obtained even at a single microwave frequency: The hyperfine limit can be inferred from the shape and intensity distribution of the correlation features over the two quadrants. Finally, HYSCORE spectra may facilitate the interpretation of lineshape singularities in case of overlapping ESEEM signals due to several nonequivalent nuclei.

REFERENCES

[1] A.V. Astashkin, S.A. Dikanov, and Yu.D. Tsvetkov. *Chem. Phys. Lett.*, 122:259, 1985.

[2] A. de Groot, R. Evelo, and A.J. Hoff. *J. Magn. Reson.*, 66:331, 1986.

[3] C.P. Lin, M.K. Bowman, and J.R. Norris. *J. Chem. Phys.*, 85:56, 1986.

[4] E.J. Reijerse and C.P. Keijzers. *J. Magn. Reson.*, 71:83, 1987.

[5] A.V. Astashkin, S.A. Dikanov, and Yu.D. Tsvetkov. *Chem. Phys. Lett.*, 136:204, 1987.

[6] A. Lai, H.L. Flanagan, and D.J. Singel. *J. Chem. Phys.*, 89:7161, 1988.

[7] S.A. Dikanov, A.V. Astashkin, and Yu.D. Tsvetkov. *Chem. Phys. Lett.*, 144:251, 1988.

[8] E.J. Reijerse and S.A. Dikanov. *J. Chem. Phys.*, 95:836–845, 1991.

[9] W.B. Mims. *Phys. Rev.*, 5:2409–2419, 1972.

[10] A.V. Astashkin, S.A. Dikanov, Yu.D. Tsvetkov, and M.G. Goldfeld. *Chem. Phys. Lett.*, 134:439, 1987.

[11] C.P. Lin and J.R. Norris. *FEBS Letters*, 197:281, 1986.

[12] A.V. Astashkin, S.A. Dikanov, A.M. Tyryshkin, and Yu.D. Tsvetkov. *Chem. Phys. Lett.*, 164:299, 1989.

[13] A.V. Astashkin, S.A. Dikanov, and Yu.D. Tsvetkov. *Chem. Phys. Lett*, 144:259, 1988.

[14] P. Höfer, A. Grupp, H. Nebenfür, and M. Mehring. *J. Chem. Phys.*, 132:279–282, 1986.

[15] E.J. Reijerse, J. Shane, E. de Boer, P. Höfer, and D. Collison. In N.D. Yordanov, editor, *Electron Magnetic Resonance of Disordered systems*. World Scientific, Singapore, 1991.

[16] J.J. Shane, P. Höfer, E.J. Reijerse, and E. de Boer. To be published. 1991.

[17] C. Gemperle, G. Aebli, A. Schweiger, and R.R. Ernst. *J. Magn. Reson.*, 88:241–256, 1990.